AMERICAN SOCIETY FOR MICROBIOLOGY | Applied and Environmental Microbiology®

ENVIRONMENTAL MICROBIOLOGY

Dicer and Argonaute Genes Involved in RNA Interference in the Entomopathogenic Fungus *Metarhizium robertsii*

Huimin Meng,[a,b] Zhangxun Wang,[a,c] Yulong Wang,[a] Hong Zhu,[a] Bo Huang[a]

Anhui Provincial Key Laboratory of Microbial Pest Control, Anhui Agricultural University, Hefei, China[a]; Shandong Provincial Key Laboratory of Synthetic Biology, Qingdao Institute of Bioenergy and Bioprocess Technology, Chinese Academy of Sciences, Qingdao, China[b]; School of Plant Protection, Anhui Agricultural University, Hefei, China[c]

ABSTRACT RNA interference (RNAi) is a gene-silencing mechanism that plays an important role in gene regulation in a number of eukaryotic organisms. Two core components, Dicer and Argonaute, are central in the RNAi machinery. However, the physiological roles of Dicer and Argonaute in the entomopathogenic fungus *Metarhizium robertsii* have remained unclear. Here, the roles of genes encoding Dicer (*M. robertsii dcl1* [*Mrdcl1*] and *Mrdcl2*) and Argonaute (*Mrago1* and *Mrago2*) proteins in *M. robertsii* were investigated. The results showed that the Dicer-like protein MrDCL2 and Argonaute protein MrAGO1 are the major components of the RNAi process occurring in *M. robertsii*. The Dicer and Argonaute genes were not involved in the regulation of growth and diverse abiotic stress response in *M. robertsii* under the tested conditions. Moreover, our results showed that the Dicer and Argonaute gene mutants demonstrated reduced abilities to produce conidia, compared to the wild type (WT) and the gene-rescued mutant. In particular, the conidial yields in the Δ*dcl2* and Δ*ago1* mutants were reduced by 55.8% and 59.3%, respectively, compared with those from the control strains. Subsequently, for the WT and Δ*dcl2* mutant strains, digital gene expression (DGE) profiling analysis of the stage of mycelium growth and conidiogenesis revealed that modest changes occur in development or metabolism processes, which may explain the reduction in conidiation in the Δ*dcl2* mutant. In addition, we further applied high-throughput sequencing technology to identify small RNAs (sRNAs) that are differentially expressed in the WT and the Δ*dcl2* mutant and found that 4 known microRNA-like small RNAs (milRNAs) and 8 novel milRNAs were *Mrdcl2* dependent in *M. robertsii*.

IMPORTANCE The identification and characterization of components in RNAi have contributed significantly to our understanding of the mechanism and functions of RNAi in eukaryotes. Here, we found that Dicer and Argonaute genes play an important role in regulating conidiation in *M. robertsii*. Our study also demonstrates that diverse small RNA pathways exist in *M. robertsii*. The study provides a theoretical platform for exploration of the functions of Dicer and Argonaute genes involved in RNAi in fungi.

KEYWORDS Argonaute, Dicer, *Metarhizium robertsii*, RNA interference

Received 29 November 2016 **Accepted** 10 January 2017

Accepted manuscript posted online 27 January 2017

Citation Meng H, Wang Z, Wang Y, Zhu H, Huang B. 2017. Dicer and Argonaute genes involved in RNA interference in the entomopathogenic fungus *Metarhizium robertsii*. Appl Environ Microbiol 83:e03230-16. https://doi.org/10.1128/AEM.03230-16.

Editor Maia Kivisaar, University of Tartu

Address correspondence to Bo Huang, bhuang@ahau.edu.cn.

H.M. and Z.W. contributed equally to this work.

RNA interference (RNAi) is a gene silencing mechanism that plays an important role in regulating gene expression from fungi, plants, and animals, and it has become a valuable molecular tool for analyzing the functions of many genes (1, 2). The 20- to 30-nucleotide (nt) small RNA (sRNA) molecules have emerged as powerful regulators of gene expression and genome stability via conserved eukaryotic RNAi-related pathways

(3). Dicer and Argonaute (AGO), as the two core proteins within the sRNA regulatory pathways, are involved in the initiation and maintenance of the mechanism central to this mode of gene regulation (4, 5). In the RNA-silencing pathway, Dicer cleaves long double-stranded RNA (dsRNA) into small interfering RNAs (siRNAs) (6–8) and also excises mature microRNAs (miRNAs) from pre-miRNAs in the cytoplasm (9). Generally, one strand of these sRNAs is then loaded into the RNA-induced-silencing complex (RISC), which contains AGOs. Under participation of AGOs with sequences complementary to the sRNAs, silencing then occurs by either cleavage or blocking translation of the target mRNA. Mature miRNAs and siRNAs are bound by AGOs, which participate in viral defense (10), posttranscriptional gene regulation (11), and transposon silencing (12, 13), processes which in turn affect somatic and germ line development. Both Dicer and AGO proteins are highly conserved from archaea to eukarya and expand largely in some plants and animals, and many organisms encode multiple members of the family (14). In distinct organisms, multiple AGOs and Dicers are involved in the RNAi pathway. Although these subtypes are similar to each other in amino acid sequence and structure, they participate in different sRNA regulatory pathways in regulating growth and development, as well as in response to abiotic and biotic stress (4, 15, 16). RNAi is mediated by sRNAs of about 20 to 30 nucleotides, and as the sRNAs regulators, Dicer and AGO have played an important role in this biological process (17).

In filamentous fungi, studies of *Neurospora*, *Magnaporthe*, *Trichoderma*, *Botrytis cinerea*, *Aspergillus*, and other species have provided a wealth of data supporting the notions that RNAi is widely conserved and that sRNA machinery components are involved in gene regulation, heterochromatin formation, and genome defense (18). In these fungi, gene regulation by RNAi has an important role in the growth, development, reproduction, and defense of cells against parasitic nucleotide sequences of viruses and transposons, as well as in the interactions with their hosts (19). *M. robertsii*, as a filamentous entomopathogenic fungus, is gaining prominence as an important pathogen used on a moderate scale for the biological control of several insect pests that cause important economic losses in agriculture. The application of *M. robertsii* as a biocontrol agent is a promising option in reducing the use of chemical acaricides, resulting in benefits for the environment. The technique of RNAi has been used successfully to suppress target gene expression in *Metarhizium* (20–23), and high-throughput sequencing of sRNAs in *M. robertsii* has led to the discovery of microRNA-like small RNAs (milRNAs) (24), both of which suggest the existence of the molecular machinery for the ribonucleoprotein complex known as the RISC in *M. robertsii*. However, as two core components in the RNAi machinery, Dicer and AGO in *M. robertsii* have physiological roles that remain unclear.

Currently, the genome sequence data on the assembled draft genome sequence of *M. robertsii*, which provides a basis of identifying RNA silencing-associated genes in the fungus, are available (25). In the present study, the characteristics and functions of Dicer and AGO genes in *M. robertsii* were systematically investigated.

RESULTS

Characteristics and expression profiles of Dicer and Argonaute genes. We chose the sequences of Dicer-like 1/2 and QDE-1/2/3 of *Neurospora crassa* as reference sequences to retrieve their orthologs in *M. robertsii*, because Dicer and AGO were intensively studied in the model fungus *N. crassa* (26). Two Dicer-like (DCL) genes (GenBank accession numbers EFY96289.1 and EFY99337.1, named *Mrdcl1* and *Mrdcl2* [i.e., the *M. robertsii dcl1* and *dcl2* genes], respectively) and two AGO genes (accession numbers EFZ02610.1 and EFZ03314.1, named *Mrago1* and *Mrago2* [i.e., the *M. robertsii ago1* and *ago2* genes], respectively) were identified in the genome of *M. robertsii*. Bioinformatic analysis indicated that both the MrDCL1 and MrDCL2 proteins contain 5 conserved domains, including a DExD domain, a helicase C domain, a Duf283 domain, and two RNase III domains; MrDCL2 also includes a dsRNA-binding domain (DS-RBD) (Fig. 1). The MrDCL2 protein in *M. robertsii* is allied closely in the phylogenetic tree with the *Cryphonectria parasitica* DCL2 protein (see Fig. S1 in the supplemental material).

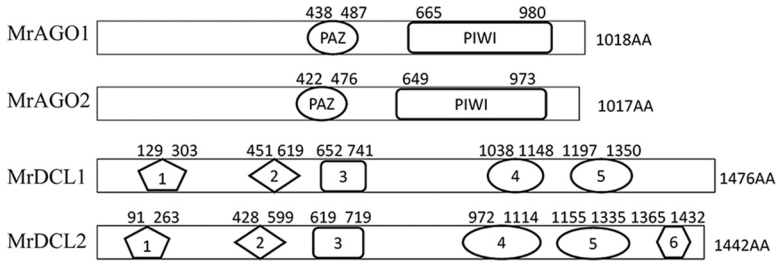

FIG 1 Peptide domain analysis of MrDCL and MrAGO proteins. 1, DExD domain; 2, helicase C domain; 3, Duf283 domain; 4, RNase III domain; 5, RNase III domain; 6, dsRNA-binding (DS-RBD) domain.

Furthermore, both the MrAGO1 and MrAGO2 proteins contain a PAZ domain and a PIWI domain (Fig. 1). The PAZ domain of MrAGO1 is composed of 50 amino acids (from residues 438 to 487) and shares 49% homology with the PAZ domain of the QDE-2 protein in *N. crassa*. The C-terminal PIWI domain of MrAGO1 includes 316 amino acids (residues 665 to 980) and has 70.4% similarity with the domain in the *N. crassa* QDE-2 protein. The PIWI domain of MrAGO2 (residues 649 to 973) shares 63.3% homology with the PIWI domain of the QDE-2 protein in *N. crassa*. We aligned the PIWI domains of the two MrAGOs to detect whether MrAGO1 and MrAGO2 possessed the conserved catalytic residues and could potentially act as the slicer component of the RISC (Fig. S2). In the conserved DDH residues, H was replaced by aspartate in MrAGO1 and MrAGO2. Furthermore, all H798 sites in the MrAGO1/MrAGO2 group of fungi were replaced by proline, consistent with the previous studies that showed a variety of H798 residues in plants (5, 27–29) (Fig. S2). Moreover, the MrAGO1 and MrAGO2 proteins in *M. robertsii* are closely allied in the phylogenetic tree with the *N. crassa* QDE-2 protein and *C. parasitica* AGL2 protein, respectively (Fig. S3).

To further explore the possible roles of the genes *Mrdcl1*, *Mrdcl2*, *Mrago1*, and *Mrago2* in different developmental stages, expression profiles of *Mrdcl1*, *Mrdcl2*, *Mrago1*, and *Mrago2* in mycelial growth, early conidiogenesis, late conidiogenesis, and pure-spore stage were analyzed by quantitative reverse transcription-PCR (qRT-PCR), and the results show that the expression levels of *Mrdcl1*, *Mrdcl2*, *Mrago1*, and *Mrago2* were detected in all investigated stages (Fig. 2). In particular, the expression trends of *Mrdcl1*, *Mrdcl2*, *Mrago1*, and *Mrago2* were highly consistent in each stage, while their expression levels were stage specific. The expression of *Mrdcl1* and *Mrago1* increased

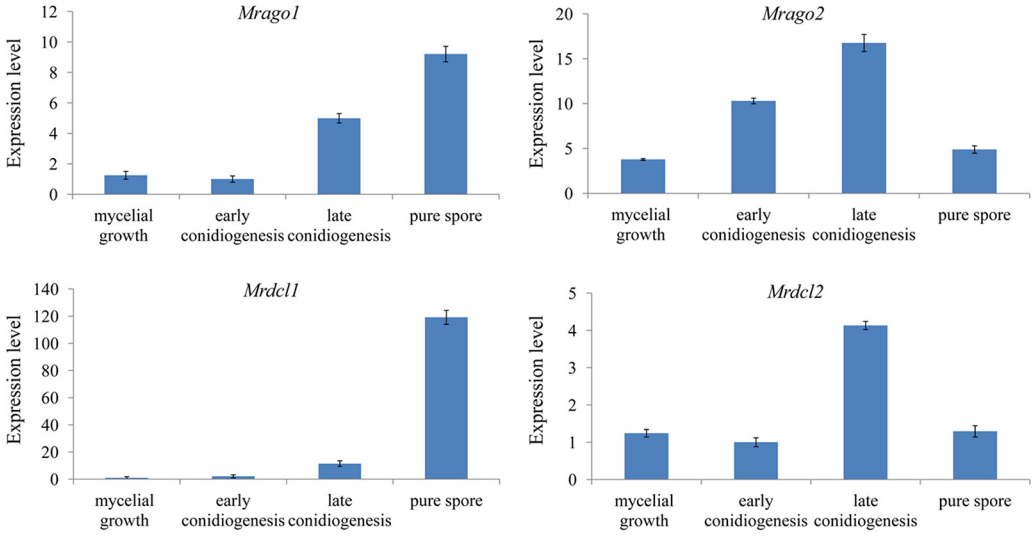

FIG 2 Expression profiles *of Mrdcl1*, *Mrdcl2*, *Mrago1*, and *Mrago2* in different developmental stages of *M. robertsii*. Data are expressed as means ± SE of values from three independent experiments. Student's *t* test was used to determine the statistical significance of differences between groups. Differences are considered significant where $P < 0.05$.

from the mycelial growth stage to the pure-spore stage, and the highest expression levels of the genes were seen in the pure-spore stage, while the expression levels of *Mrdcl2* and *Mrago2* showed the relatively highest expression in the late-conidiogenesis stage.

Disruption and complementation of Dicer and AGO. To characterize the physiological functions of the Dicer and AGO genes in *M. robertsii*, we generated gene replacement mutants for each gene using different dominant selectable marker genes, *BAR* or *BEN*, as described in Materials and Methods.

The Δ*dcl1*, Δ*dcl2*, Δ*ago1*, and Δ*ago2* gene deletion mutants, in which the named genes were inserted into the binary vectors pBar-dcl1, pBen-dcl2, pBar-ago1, and pBen-ago2, respectively, were constructed by replacing the coding regions with the *BAR* or *BEN* gene cassette.

We also constructed a Δ*ago1* Δ*ago2* double mutant strain and a Δ*dcl1* Δ*dcl2* double mutant strain for further functional analysis of Dicer and Argonaute genes. The Δ*dcl1* Δ*dcl2* mutant was constructed by replacing the coding region of *Mrdcl1* in the Δ*Mrdcl2* mutant with the binary vector pBar-dcl1, and the Δ*ago1* Δ*ago2* mutant was constructed by replacing the coding region of *Mrago1* in the Δ*Mrago2* mutant with the binary vector pBar-ago1.

Complementation strains (the cpΔ*dcl1*, cpΔ*dcl2*, cpΔ*ago1*, and cpΔ*ago2* strains) were obtained by transforming cpBen-dcl1, cpBar-dcl2, cpBen-ago1, and cpBar-ago2 into the Δ*dcl1*, Δ*dcl2*, Δ*ago1*, and Δ*ago2* mutants, respectively. All the recombinant strains were confirmed by PCR and reverse transcription-PCR (RT-PCR) (Fig. S4A to C).

Roles of Dicers and AGOs in asexual reproduction. The growth rates of Dicer and AGO mutants were examined by incubating wild-type (WT) and mutant cultures at 25°C on Sabouraud-dextrose-yeast extract agar (SDAY) medium. All deletion mutants exhibited growth rates and phenotypic characteristics similar to those of the WT (data not shown). Osmotic, oxidative, and cell wall effects were examined on plates containing NaCl, H_2O_2, and SDS, respectively, with the data presented as the percentage of growth inhibition (GI). Contrary to our expectations, the GI of the Dicer and AGO mutants in the presence of stressful chemicals was not significantly different from that shown by the control strains (data not shown).

However, when conidia from the WT, the mutants, and the complemented mutants (control strains) were quantified, the results showed that the conidial yields in the Δ*dcl1*, Δ*dcl2*, Δ*dcl1* Δ*dcl2*, Δ*ago1*, Δ*ago2*, and Δ*ago1* Δ*ago2* mutants were reduced by 27.0%, 55.8%, 40.2%, 59.3%, 46.0%, and 56.8%, respectively, compared with those from the control strains, which indicated a significant reduction of conidial yield in each deletion mutant, especially in the Δ*dcl2* and Δ*ago1* mutants, compared with the yield of the WT (Fig. 3). The data may suggest that *Mrdcl2* and *Mrago1* are the major genes responsible for regulating conidiation compared with *Mrdcl1* and *Mrago2*, respectively. These results indicate a role for Dicer and AGO in the regulation of asexual development in *M. robertsii*.

***Mrdcl2* regulates the transcriptional response during conidiation.** Because Dicers are upstream in the RNAi pathway in charge of generating sRNAs by processing double-stranded RNA precursors, the conidial yield of the Δ*dcl2* mutant is significantly decreased. Therefore, to further elucidate the possible mechanism involved in the sporulation of *M. robertsii* affected by the *Mrdcl2* gene, we examined the set of differentially expressed genes (DEGs) for mycelial growth (MY; conidia grown on SDAY for 1 day) and conidiogenesis (CO; mycelia grown on SDAY for 2.5 days) in the WT and the Δ*dcl2* mutant. The results show that a total of 4,264 differentially expressed genes (3,065 genes upregulated and 1,199 genes downregulated) for the WT and 4,397 genes (3,082 genes upregulated and 1,315 genes downregulated) for the Δ*dcl2* mutant were detected (Table S1). The expression of a number of these downregulated genes, such as those for cyclin-like protein (GenBank accession number MAA_00500), ATP-dependent DNA helicase PIF1 (MAA_10537), pyruvate carboxylase subunit A (MAA_01657), and the propionyl-coenzyme A (propionyl-CoA) carboxylase beta chain

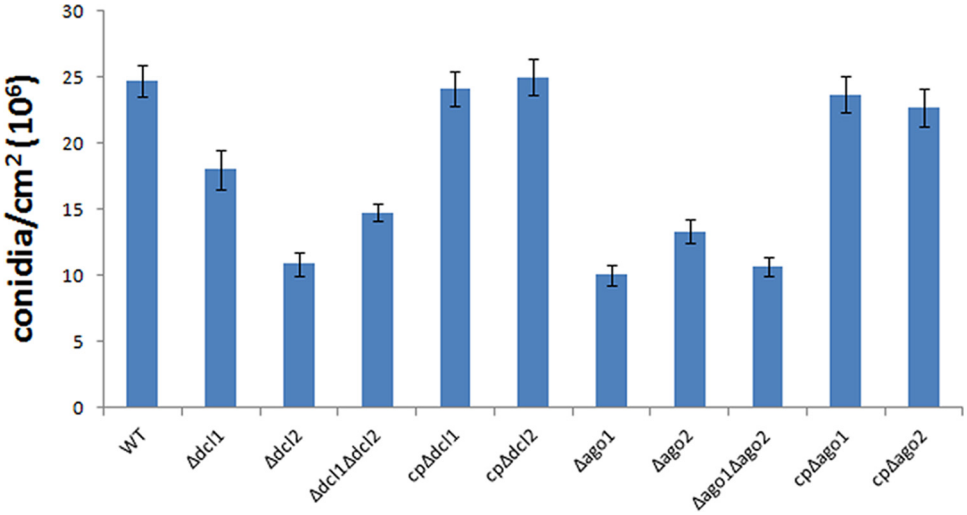

FIG 3 Production of conidia of the WT and the *Mrdcl1*, *Mrdcl2*, *Mrago1*, and *Mrago2* deletion mutants. Data are expressed as means ± SE of values from three independent experiments. Student's *t* test was used to determine the statistical significance of differences between groups. Differences are considered significant where $P < 0.05$.

(MAA_01658), is increased in the Δ*dcl2* mutant, suggesting that those drastically suppressed genes were likely responsible for the sporulation defections in the Δ*dcl2* mutant.

To validate the differentially expressed genes detected by RNA sequencing (RNA-seq) data, we tested them by qRT-PCR in a different biological replicate. Overall, the 18 selected genes were successfully validated (Table 2).

Enrichment analysis of gene ontology (GO) terms for DEGs in the WT and the Δ*dcl2* mutant was conducted to clarify which processes are more relevant to conidiation in *M. robertsii*. The results indicated that the upregulated genes are significantly enriched ($P < 0.05$) in 31 GO categories in both the WT and the Δ*dcl2* mutant. Interestingly, the downregulated genes in the WT are significantly enriched in 54 GO categories (23 in biological processes, 18 in molecular functions, and 13 in cellular components), while those in the Δ*dcl2* mutant are significantly enriched in 85 GO terms (39 in biological processes, 21 in molecular functions, and 25 in cellular components) (Table S2). Furthermore, we found that 2,263 upregulated and 713 downregulated genes are shared by the two strains by comparing the DEGs from the WT and the Δ*dcl2* strains (Fig. 4A and Table S3). The upregulated genes are involved mostly in processes such as the oxidation-reduction process (GO:0055114), transmembrane transport (GO:0055085), and the carbohydrate metabolic process (GO:0005975), while the downregulated genes are involved mainly in processes such as translation (GO:0006412), ribosomal biogenesis (GO:0042254), rRNA processing (GO:0006364), and mycelium development (GO:0043581). The results indicated that the DEGs in the Δ*dcl2* mutant might affect the regulation of the conidiation in *M. robertsii* (Fig. 4A and Table S3).

As a result of surveying genes, 1,288 genes (802 upregulated and 486 downregulated genes) were found to be differentially expressed only in the WT (group I), and at least some of them, such as those for cytochrome P450 CYP5148B3 (GenBank accession number MAA_01512; fold change, 11.0), flavin adenine dinucleotide (FAD) binding domain-containing protein (MAA_07499; fold change, 11.95), and fungus-specific transcription factor (MAA_09943; fold change, 11.1), may be required for conidiation in *M. robertsii*. To a certain extent, the DEGs (819 upregulated and 602 downregulated genes) found only in the Δ*dcl2* mutant (group II), including those for cytochrome b_5 reductase protein (MAA_08854; fold change, 12.4), polyketide synthase (MAA_08549; fold change, −10.2), and TRI14-like protein (MAA_00154; fold change, 12.1), might inhibit the sporulation of *M. robertsii*. It is interesting to note that the number of group II downregulated genes that were involved in enrichment in GO terms was much larger than that in group I (Fig. 4B and C).

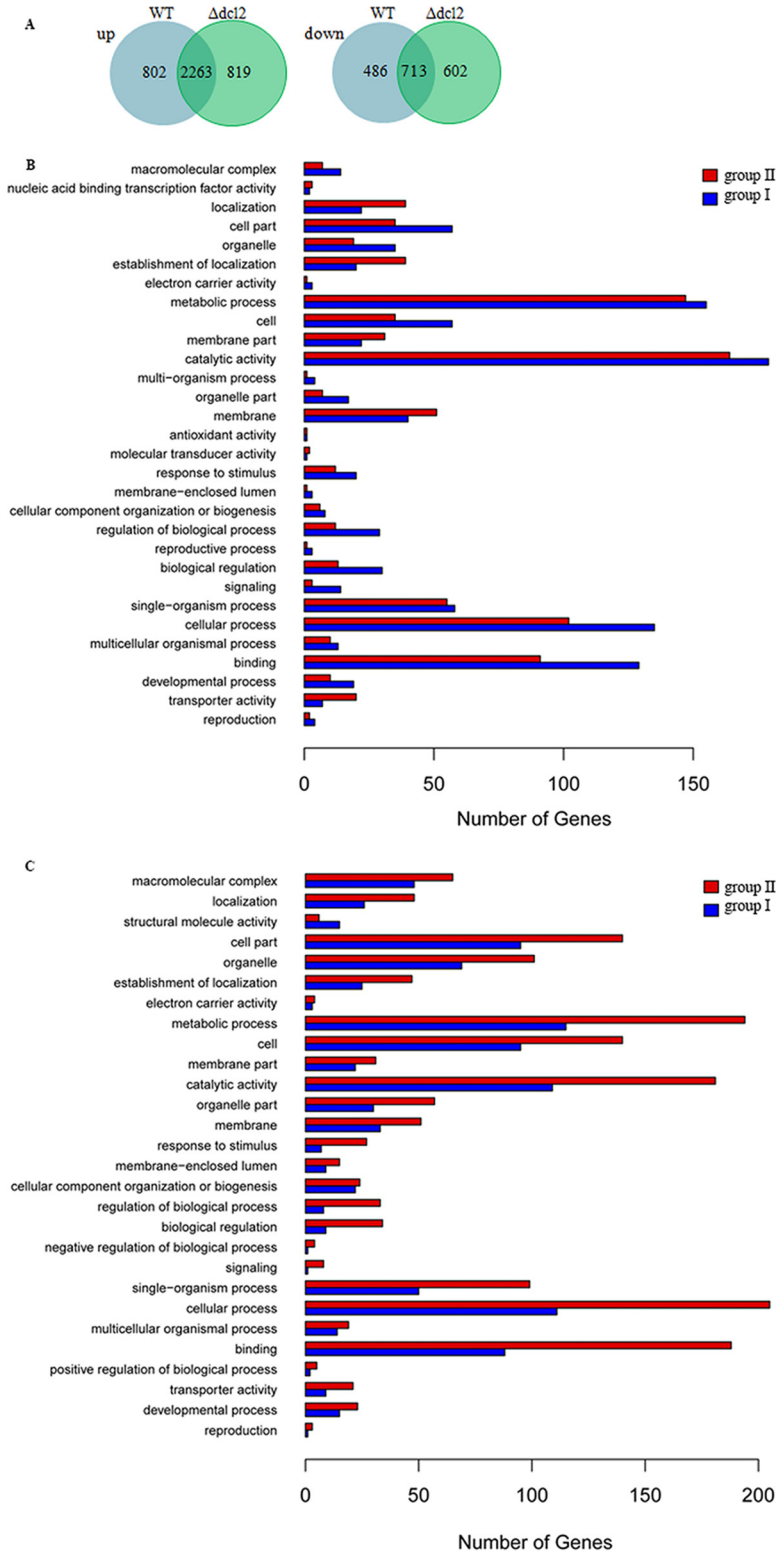

FIG 4 Analysis of the differentially expressed genes in the WT and Δ*dcl2* strains. (A) Overlap between upregulated (up) and downregulated (down) genes in the WT and Δ*dcl2* mutant strains; (B and C) GO terms of upregulated (B) and downregulated (C) genes of group I (specific for the WT) and group II (specific for the Δ*dcl2* mutant).

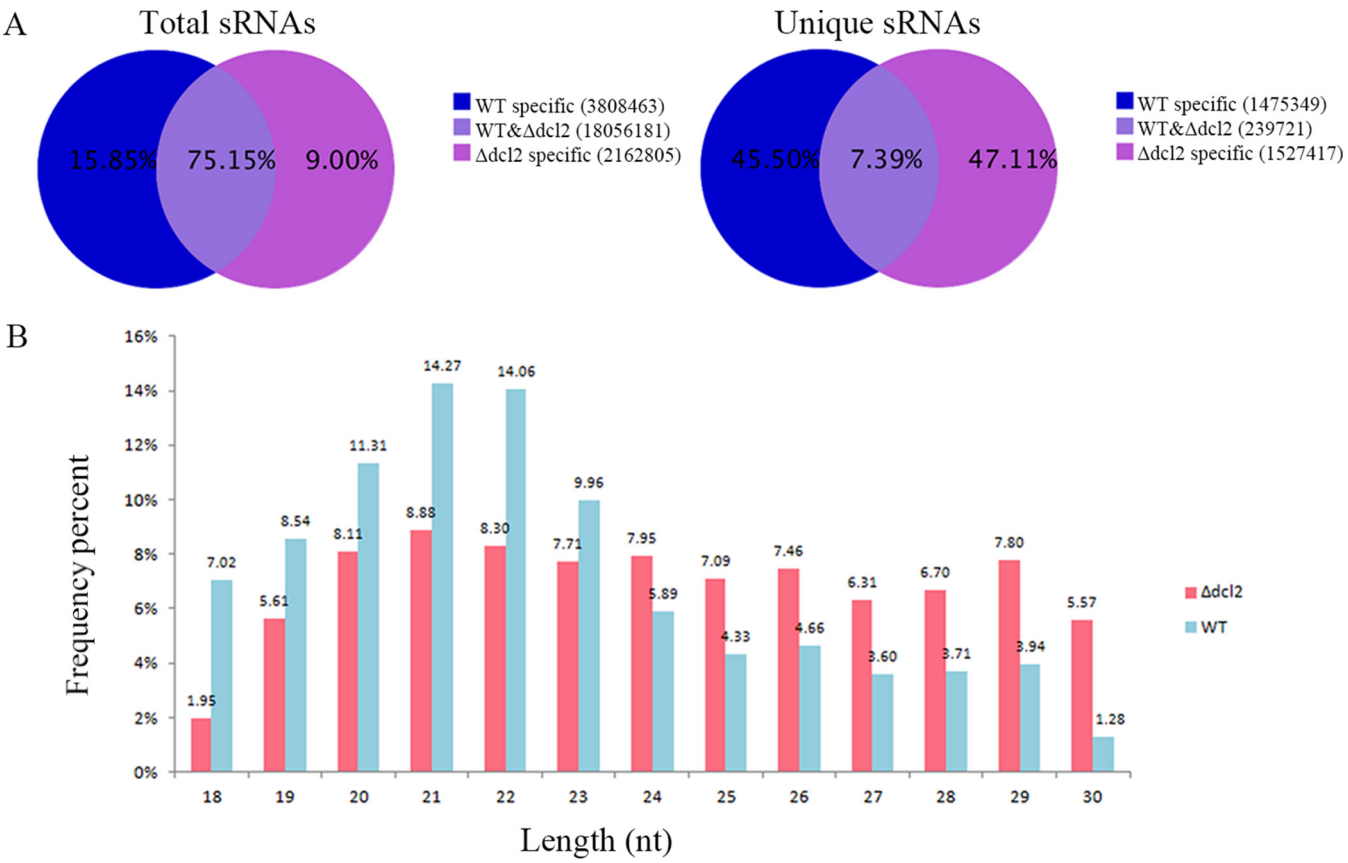

FIG 5 Characteristics of small RNAs from the WT and Δ*dcl2* mutant strains. (A) Proportion of the public and special sequences of sRNAs; (B) size distribution of small RNAs.

***Mrdcl2* is involved in the biogenesis of small RNAs.** Combined with the results of phenotype and bioinformatic analyses, we speculated that *Mrdcl2* may be the major gene involved in sRNA biosynthesis, compared with *Mrdcl1* in *M. robertsii*.

Here, to further examine sRNAs that may be generated by the *Mrdcl2* gene of *M. robertsii*, we constructed cDNA libraries of sRNAs from both the WT and Δ*dcl2* mutant strains. After removal of the barcode and exclusion of sequences that were shorter than 18 nucleotides, totals of 11,404,976 and 12,622,473 clean reads were obtained from the WT and the Δ*dcl2* mutant, respectively (Table S4). The unique sRNAs in the WT differed significantly from those in the Δ*dcl2* mutant, and only 7.39% of unique sRNAs were shared by both the WT and Δ*dcl2* mutant strains (Fig. 5A). These reads were mapped to the *M. robertsii* genome, and they coincided with a variety of genomic features, including tRNAs, rRNAs, small nuclear RNAs (snRNAs), and small nucleolar RNAs (snoRNAs) (Table S5). We found that the sRNAs identified from both the WT and Δ*dcl2* mutant strains were 18 to 30 nt in length, consistent with the range of lengths previously observed for sRNAs in fungi. The sRNAs of the selected population peaked at 21 nt in length, reaching 14.27% in the WT and only 8.88% in the Δ*dcl2* mutant (Fig. 5B).

In addition, by analyzing the 5′-nucleotide bias in sRNAs, especially sRNAs of 21 nt, we observed that uracil (U) was more frequently found at their 5′ end in the WT and that this bias was guanine (G) in the Δ*dcl2* mutant (Fig. 6A and B). As shown in Fig. 6C and D, it is clear that the nucleotide biases at every position of the sRNAs differ significantly between the WT and the Δ*dcl2* mutant. Furthermore, analysis of the distributions of sRNAs on chromosomes showed that the sRNAs from the WT and the Δ*dcl2* mutant have distinct chromosomal distributions (Fig. S5). These results showed that the sRNAs differ in their modes of biogenesis in the Δ*dcl2* mutant and the WT, which indicated that *Mrdcl2* plays an important role in sRNA biogenesis in *M. robertsii*.

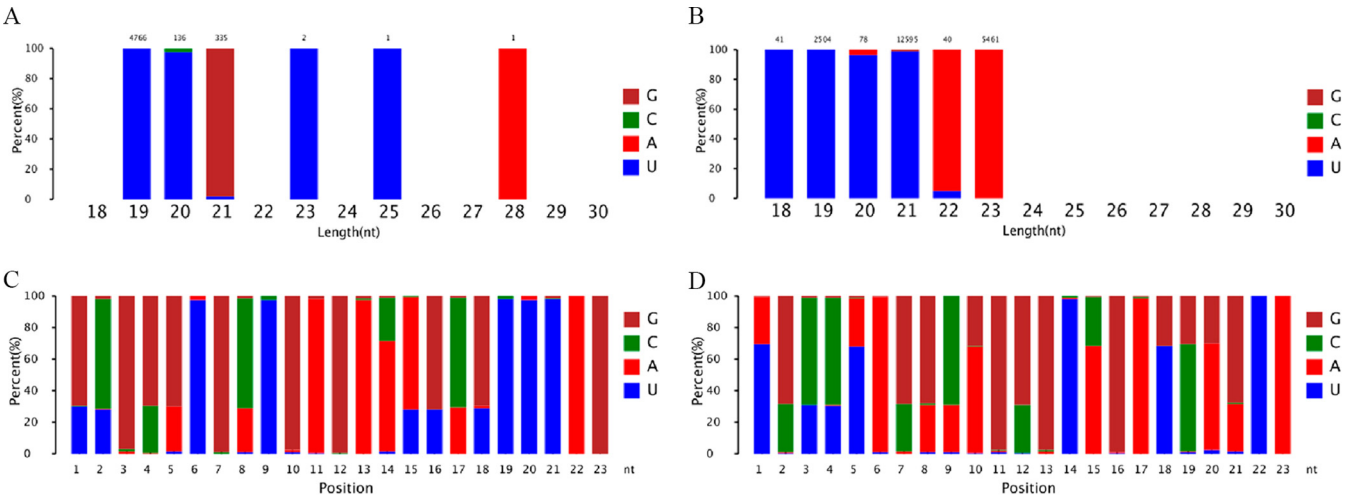

FIG 6 Analysis of nucleotide biases of sRNAs. (A and B) 5′-end nucleotide biases of 18- to ~30-nt sRNAs in the Δ*dcl2* mutant (A) and WT strain (B); (C and D) nucleotide bias at each position of sRNAs in the Δ*dcl2* mutant (C) and WT strain (D).

It has been reported that several milRNAs were identified in *M. robertsii* by our laboratory (24); therefore, the expression of these milRNAs was further investigated in the WT and the Δ*dcl2* mutant. As shown in Fig. 7 and Table S6, 4 known milRNAs and 8 novel milRNAs were not detected in the Δ*dcl2* mutant, indicating that these milRNAs might be *Mrdcl2* dependent. The expression levels of milRNA-1 and milRNA-8 did not change significantly between the Δ*dcl2* mutant and the WT. Interestingly, 1 known milRNA (man-milR-12) and 4 novel milRNAs were identified in the Δ*dcl2* mutant but not in the WT. These results suggested that *Mrdcl2* was involved in milRNA biosynthesis in *M. robertsii*.

DISCUSSION

RNAi is a conserved eukaryotic gene silencing mechanism in the regulation of gene expression at both the posttranscriptional and transcriptional levels. Here, Dicers and AGOs, as core proteins of RNAi, were analyzed and characterized from *M. robertsii*.

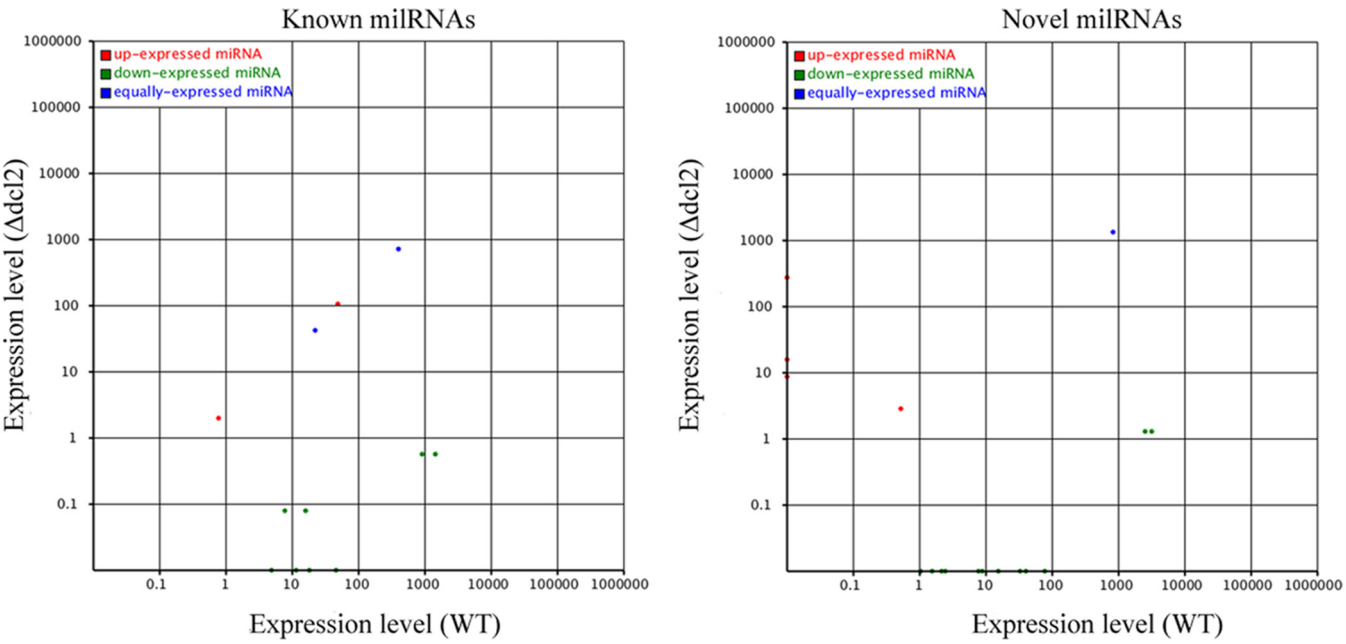

FIG 7 Comparisons of expression levels of milRNAs in the WT and Δ*dcl2* mutant.

Phylogenetic trees were constructed using the neighbor-joining method and plotted with MEGA, showing that MrDCL2 in *M. robertsii* was clustered in the phylogenetic tree with Dicer2 of *N. crassa*, an RNase III-like enzyme central to the majority of sRNA generation pathways (Fig. S1). Moreover, the MrAGO1 protein in *M. robertsii* is allied closely in the phylogenetic tree with *N. crassa* QDE-2, a canonical AGO protein (Fig. S3). Many studies have revealed that Dicer-like proteins are evolutionarily conserved in many eukaryotic organisms. Previous studies indicated that MDL-2 has a distinct role in siRNA accumulation, and no functional redundancy exists between MDL-1 and MDL-2 in the RNA-silencing pathway in *Magnaporthe oryzae*, which is similar to the results obtained with *Drosophila melanogaster* (30, 31). However, the two Dicer-like proteins appear redundant in transgene-induced posttranscriptional gene silencing in *N. crassa* (32). Many genes, such as Dicer, AGO, and RNA-dependent RNA polymerase (RdRp), involved in the sRNA regulatory RNAi pathway were expressed at different development stages or in specific organs, or both, which provides information regarding their functions (27). In the present study, we analyzed the expression of Dicers by relative qRT-PCR at different developmental stages of *M. robertsii*. The upregulation expression of *Mrdcl2* at the late-conidiogenesis stage may suggest that *Mrdcl2* is involved in the RNAi pathway to regulate gene expression in that stage. Based on the results of sequence analysis and qRT-PCR analysis, we speculated that *Mrdcl2*, not *Mrdcl1*, is the major Dicer gene that processes dsRNA into siRNA in the RNAi mechanism in vegetative growth and development, which is consistent with what occurs in most fungi (30, 32, 33).

Phenotypic analyses of yeasts and filamentous fungi with mutations in RNAi pathway components have revealed that although RNAi may play important roles in various aspects of development, homeostasis, and disease, its functions may vary significantly among different fungal species. In this study, to further investigate the potential roles of Dicers and AGOs (including *Mrago1*, *Mrago2*, *Mrdcl1*, and *Mrdcl2*), gene deletion and complementation were performed via *Agrobacterium*-mediated transformation, and the resultant strains were analyzed by PCR and RT-PCR. The results showed that all deletion mutants exhibited growth rates and colony morphology on SDAY or various environmental-stress media (including NaCl, H_2O_2, and SDS) similar to those of the WT strain (data not shown). This suggests that in *M. robertsii*, the RNAi machinery is not involved in the regulation of vegetative growth and diverse stress responses under the tested conditions. Moreover, we found that sporulation of all mutants was impaired. In particular, the conidial yields in the Δ*dcl2* and Δ*ago1* mutants were reduced by 55.8% and 59.3%, respectively, compared with those of control strains. This is consistent with what has been observed in *Trichoderma atroviride* (34).

Transcriptomic analysis at the genome-wide level is a valuable tool to identify differentially expressed genes that are regulated by signaling pathways. For instance, digital gene expression (DGE) profiling revealed that genes involved in cell wall construction, conidiation, stress tolerance, cell cycle control, and calcium transport were downregulated in a mutant of *Metarhizium acridum* with a deletion of *Cna* (35). In the present study, to explore the underlying mechanism of effect on the sporulation by *Mrdcl2*, we used RNA-seq to systematically investigate differentially expressed genes that are regulated by *Mrdcl2* during the MY and CO stages of *M. robertsii*. The results show that altered expression levels of genes, such as cyclin-like protein (GenBank accession number MAA_00500), cytochrome b_5 reductase protein (MAA_08854), and TRI14-like protein (MAA_00154), may explain the phenotypes observed in reproductive growth in *Mrdcl2* mutants. It has been reported that conidiation was associated with a coordinated downregulation of the expression of genes encoding ribosomal proteins in *Aspergillus fumigatus* (36). In agreement with this, many genes, including ribosomal protein L13 (MAA_02493), 50S ribosomal protein L14 (MAA_07112), 30S ribosomal protein S13 (MAA_06819), ribosomal protein S19 (MAA_08323), and ribosomal protein L10e (MAA_03051), encoding ribosomal proteins were repressed significantly during conidiation only in the WT and not in the Δ*dcl2* mutant. This suggests that during conidiation, there is a correlation with the synthesis of those proteins necessary

for conidiation. Especially, since many genes involved in conidiation, including *flbC*, *fluG*, *flbA*, *phiA*, *stuA*, *medA*, *wetA*, *brlA*, and *abaA*, are repressed in the Δ*dcl2* mutant compared with the WT, this suggests that the mutant is affected during conidiation. Furthermore, genes such as *wetA*, *brlA*, and *abaA* have been identified as part of a central regulatory pathway that functions with other genes to control conidiation-specific gene expression and to determine the order of gene activation during conidiophore development and spore maturation in *Aspergillus nidulans* (37). In addition, previous research revealed that two developmental regulatory genes, *stuA* and *medA*, were necessary for spore formation in *A. nidulans* (38, 39). Therefore, differential expression of several genes between the Δ*dcl2* mutant and the WT were analyzed by qRT-PCR. The results show that the same genes were repressed in the Δ*dcl2* mutant, which is consistent with the previous findings for *A. nidulans*. It suggests that these genes may also function in promoting conidiation in *M. robertsii*.

Combined with the results of bioinformatic and qRT-PCR analyses, we speculated that *Mrdcl2*, not *Mrdcl1*, is the major Dicer gene whose enzyme processes dsRNA into sRNA (miRNA or siRNA), which is consistent with what occurs in most fungi (30, 32, 33). Therefore, characteristics and expression profiles of sRNAs (18 to 30 nt in length) from the Δ*dcl2* mutant were further analyzed by high-throughput sequencing and compared to those of the WT. Our results indicated that the Δ*dcl2* mutant lost the main characteristic features of the sRNAs found in the WT. Furthermore, the 5′-nucleotide bias was different from that of the WT, which contrasts with those observed for AGO-bound guide sRNAs in other fungi (40–42). Moreover, several sRNAs show differential expression in the Δ*dcl2* mutant and WT, which suggests that the sRNAs generated by *Mrdcl2* may be associated with the regulation of conidiation in *M. robertsii* (see Table S6 in the supplemental material). In particular, milRNAs, including those in *N. crassa* (40), *Penicillium marneffei* (43), *Sclerotinia sclerotiorum* (44), and *Fusarium graminearum* (45), have been identified, and they have an important function in regulating different biological processes in these fungi. Previously, it was discovered by our group that milRNAs may play an important role in the regulation of conidiation in *M. robertsii* (24). In the present study, differential expression of milRNAs in WT and the Δ*dcl2* mutant was further investigated, and the results show that a total of 4 known milRNAs and 8 novel milRNAs dependent on *Mrdcl2* were identified from sRNAs. Intriguingly, 4 novel milRNAs were found in the Δ*dcl2* mutant but not in the WT; that is, biosynthesis of the 4 milRNAs is independent of *Mrdcl2*, which indicates that a diverse small RNA pathway exists in *M. robertsii*. Indeed, a previous report indicated that there are at least four different pathways for milRNA production in the model fungus *N. crassa*, which required a distinct combination of Dicers, QDE-2, the exonuclease QIP, and an RNase III domain-containing protein, MRPL3 (40). Thus, further investigations should be considered to explore the biological functions of these proteins in milRNAs through experimental approaches in *M. robertsii*.

MATERIALS AND METHODS

Fungal strains and culture conditions. *M. robertsii* strain ARSEF 23 was kindly provided by Chengshu Wang. Conidia were obtained from potato dextrose agar at 25°C for 12 days, cultured (10^7 conidia/ml; the same below unless mentioned otherwise) onto cellophane (0.5-μm pore) on SDAY, and incubated at 25°C. Fungal biomass was harvested at 1.5 days (mycelial growth), 2 days (early conidiogenesis), 3 days (late conidiogenesis), and 12 days (pure-spore stage) after incubation.

Sequence retrieval and phylogenetic analyses of Dicer and AGO families. *M. robertsii* genome and transcriptome sequence data were downloaded from the NCBI (http://www.ncbi.nlm.nih.gov/). The BLASTp algorithm, underpinned by the Pfam and CDD databases, was used for searches of conserved protein domains or motifs.

The amino acid sequences of Dicer and AGO proteins from *M. robertsii* and other organisms obtained from GenBank were aligned using CLUSTALW (46). Phylogenetic trees were constructed using the neighbor-joining method and plotted with MEGA (47).

qRT-PCR analysis of *Mrdcl1*, *Mrdcl2*, *Mrago1*, and *Mrago2* transcription in different developmental stages of *M. robertsii*. Total RNAs from different developmental stages of *M. robertsii* were isolated using TRIzol reagent (Invitrogen, USA). Nucleic acid concentrations were measured with an ND-1000 spectrophotometer (NanoDrop, USA), and 1 μg of RNA was reverse transcribed using the PrimeScript first-strand cDNA synthesis kit (TaKaRa, China). Reverse-transcribed cDNA samples were used as the template for qRT-PCR amplification using SYBR green (TaKaRa, China) and a 7500 real-time PCR

TABLE 1 Sequences of primers used

Category and gene	Primer name	Sequence (5′ to 3′)	Notes
Gene replacement			
Mrdcl1	Mrdcl1-5F	CGGAATTCGCGAAACAACAGCCAGAGTA	
	Mrdcl1-5R	CGGGATCCGCAAACAACCCAGACCAGA	
	Mrdcl1-3F	GGACTAGTTCGATTTAGTGGGAATGAGC	
	Mrdcl1-3R	GCTCTAGACATCGCTTGAATCTCCTGTG	
	Mrdcl1-NF	TTGATTGCGATTCGGGTAG	PCR identification of *Mrdcl1* deletion transformants
	Mrdcl1-NR	CGTCAACATCCTCCTCACC	
Mrdcl2	Mrdcl2-5F	AACTGCAGCAAAGGTTCCTCGCCAGTCC	
	Mrdcl2-5R	AACTGCAGATCCCGCCATTCAACTAACG	
	Mrdcl2-3F	GGACTAGTCAGAAACAGCCGTTACATCC	
	Mrdcl2-3R	GCTCTAGAGCTCTGCCATTATTCTTGTCG	
	Mrdcl2-NF	CCGACACCTGGGATACGAT	PCR identification of *Mrdcl2* deletion transformants
	Mrdcl2-NR	AGTTGCTCGCTCCTTTACG	
Mrago1	Mrago1-5F	CGGAATTCATCGCTTCCCGACTGTGA	
	Mrago1-5R	CGGGATCCTGGCCGCTGCTGCTAAAT	
	Mrago1-3F	GGACTAGTTGGTCTCGTCGCTTCTGT	
	Mrago1-3R	GCTCTAGATGCTTGGGCATCGACTTG	
	Mrago1-NF	TCCCGAGACACTGATAGGC	PCR identification of *Mrago1* deletion transformants
	Mrago1-NR	CAACGACTTATGGACCTG	
Mrago2	Mrago2-5F	AACTGCAGTTGACCTCGGTGCTTTCG	
	Mrago2-5R	AACTGCAGGGCGCTGAGGGTTGCTAT	
	Mrago2-3F	GGACTAGTAGTCGGATATTGTGAAAGCG	
	Mrago2-3R	GCTCTAGACCTTTGGCTTGTATGTCTGC	
	Mrago2-NF	ATGTCTAGTGGGCATAGAGGTG	PCR identification of *Mrago2* deletion transformants
	Mrago2-NR	AGCTGCTGAGCTGTCTGG	
BAR	bar-F	GGAGGTCAACAATGAATGCC	
	bar-R	CCACGTCATGCCAGTTCC	
BEN	ben-F	ATGGCTACCTACTCCGTCGTG	
	ben-R	CTCGTCCATACCCTCACCA	
Gene complementation			
Mrdcl1	Mrdcl1cp5F	GCTCTAGAGCGAAACAACAGCCAGAG	
	Mrdcl1cp3R	GCTCTAGATCCCGTCGTGTTCTTCTT	
Mrdcl2	Mrdcl2cp5F	GCTCTAGAGCCAAGGCAGTGAAGTAT	
	Mrdcl2cp3R	GCTCTAGACTGCCATTATTCTTGTCG	
Mrago1	Mrago1cp5F	GCTCTAGAGACGAAAGAGGCATACACT	
	Mrago1cp3R	GCTCTAGACTGCTTGGGCATCGACTT	
Mrago2	Mrago2cp5F	GCTCTAGAGGTCACCAAATTGCACCTA	
	Mrago2cp3R	GCTCTAGAGAGCCACTGCCAGTATAAGT	
Gene expression analysis and RT-PCR identification of deletion transformants			
Mrdcl1	Mrdcl1F	GAAGGCGGTCACTGTAATGG	
	Mrdcl1R	ATGGGTATGACGGATGCTTG	
Mrdcl2	Mrdcl2F	CCGACTTCCTTCATCCTGTT	
	Mrdcl2R	TTCGCAATCAATGTGACCTC	
Mrago1	Mrago1F	GAGAAGACCGAAGTAAAGGATG	
	Mrago1R	CGGACGGAATGTTGATAGTG	
Mrago2	Mrago2F	GCATCAATCAGACGGTGGAG	
	Mrago2R	ATTAGAGGAGGAGCCAGGTGAG	
gpd	gpdF	GACTGCCCGCATTGAGAAG	
	gpdR	AGATGGAGGAGTTGGTGTTG	

system (Applied Biosystems). Specific primers for the *M. robertsii* glyceraldehyde 3-phosphate dehydrogenase (*gpd*) gene (GenBank accession number MAA_07675) were used as an internal control for normalization (48). The cDNAs from three biological samples were used for analysis, and all the reactions were run in triplicate. qRT-PCR was performed using 1 μl of cDNA in a final volume of 10 μl containing 5 μl of 2× SYBR *Premix Ex Taq* II, 0.2 μl of ROX reference dye II, and 0.4 μl of specific primers for each AGO and Dicer (10 μM) (Table 1), with the following thermal cycling profile: 95°C for 30 s, followed by 40 cycles of amplification (95°C for 5 s, 60°C for 34 s). The threshold cycle (C_T) was determined using the default threshold settings. Melting curves were also measured for the specificity of primers. Relative expression was calculated according to the $2^{-\Delta\Delta CT}$ method (49).

Gene deletion and complementation. Targeted gene deletion of *Mrdcl1*, *Mrdcl2*, *Mrago1*, and *Mrago2* genes was performed by homologous recombination via *Agrobacterium*-mediated fungal transformation, according to the procedure of Wang et al. (50), and pDHt-SK-bar/pDHt-SK-ben vectors were also kindly provided by Chengshu Wang (50, 51). Briefly, the 5′- and 3′-end-flanking regions of *Mrdcl1*

were amplified using the Dream *Taq* DNA polymerase (Fermentas, USA). The genomic DNA was used as the template in PCR along with the primer pairs Mrdcl1-5F/Mrdcl1-5R and Mrdcl1-3F/Mrdcl1-3R (Table 1), respectively. The purified 5′- and 3′-end-flanking fragments were subsequently cloned into the EcoRI/BamHI and SpeI/XbaI restriction enzyme sites in the binary vector pDHt-SK-bar (conferring resistance against ammonium glufosinate) to produce the binary vector pBar-dcl1 for *Agrobacterium*-mediated fungal transformation. *M. robertsii* transformation mediated by *Agrobacterium tumefaciens* was according to the protocol of Fang et al., with modifications, as described previously (52). *A. tumefaciens* strain AGL-1, containing pBar-dcl1, was cultured at 28°C for 16 to 20 h in yeast extract broth (YEB) medium (0.5% sucrose, 0.1% yeast extract, 0.5% peptone, 0.05% $MgSO_4 \cdot 7H_2O$) supplemented with kanamycin (50 μg/ml) and carbenicillin (50 μg/ml), with shaking at 220 rpm. The *A. tumefaciens* cells were diluted to an optical density at 660 nm (OD_{660}) of 0.15 in induction medium (IM) with or without 200 μM acetosyringone (AS). The cells were then grown in IM at 28°C with shaking at 220 rpm until an OD_{660} value of 0.5 to 0.8 was reached. *M. robertsii* conidia were harvested in 0.05% Tween 80 aqueous solution, and the conidial suspension was filtered through sterile nonwoven fabrics to remove mycelia. The working conidial concentrations were adjusted to 10^6 conidia/ml with sterile double-distilled water (ddH_2O). One hundred microliters of a conidial suspension was mixed with an equal volume of *A. tumefaciens* cells in IM (OD_{660} = 0.5 to 0.8) with or without AS. The mixture (200 μl per plate) was spread on IM agar plates in the presence or absence of AS. After cocultivation at 28°C for 48 h, the cellophane sheet was transferred to M-100 plates containing ammonium glufosinate (200 μg/ml) as a selection agent for transformants and cefotaxime (300 μg/ml) to kill the *A. tumefaciens* cells and was incubated at 28°C. Putative transformants were visible at approximately 7 days. Individual transformants were transferred into SDAY plates for further analysis.

For mutant complementation, the *Mrdcl1* gene was amplified together with the promoter region and terminator region using the primer pair Mrdcl1cp5F/Mrdcl1cp3R, and the product was digested with XbaI and then inserted into the binary vector pDHt-SK-ben (conferring resistance against benomyl) to transform the Δ*dcl1* mutant for obtaining the complement strain.

Transformants were verified by PCR, and RT-PCR analysis was performed using the primer pair Mrdcl1F/Mrdcl1R (Table 1). The *gpd* gene was used as an internal control.

Deletions of the *Mrdcl2*, *Mrago1*, and *Mrago2* genes were performed by using the same method, and all primers used are listed in Table 1. To generate Dicer and AGO double mutants, the gene replacement constructs for *Mrdcl1* and *Mrago1* were transformed to the Δ*dcl2* and Δ*ago2* mutants, respectively. The double-knockout mutants were also verified by PCR and RT-PCR analyses with the primers (Table 1).

Assays for cellular responses to chemical stresses. To investigate the cellular responses on chemical stresses, 2-μl aliquots of conidial suspension were centrally spotted onto the plates of SDAY alone (control) or supplemented with a sensitive concentration of H_2O_2 (2 mM) for oxidative stress, SDS (0.025%) for cell wall perturbation, and NaCl (1 M) for hyperosmotic stress. After cultivation at 25°C for 7 days, the mean diameter of each fungal colony was cross-measured in each stress treatment plate and the control (chemical-free) plates.

Sporulation assay. To assay the sporulation capacity of the WT and each mutant, 40-μl aliquots of conidial suspension were evenly spread on SDAY plates (35-mm diameter) and incubated for 7 days at 25°C and 12-h/12-h light/dark cycle. The conidia on each plate were harvested in 20 ml of 0.05% Tween 80 and vortexed adequately, and the conidial suspension was filtered through sterile nonwoven fabrics to remove mycelial debris. The conidial concentration in the suspension was counted with a hemocytometer and converted to the number of conidia per square millimeter of colony. This experiment was carried out in triplicate and repeated, with similar results obtained.

Digital gene expression profile analysis of the WT and Δ*dcl2* mutant. Conidia of the WT and the Δ*dcl2* mutant were inoculated into SDAY medium at 1×10^7 conidia/ml. Fungal samples were collected after 1 day (mycelial growth [MY]) and 2.5 days (conidiogenesis [CO]). Total RNA was extracted using TRIzol reagent (Invitrogen, New York, NY, USA), according to the manufacturer's instructions. Total RNA (5 μg) was prepared for Illumina RNA-Seq, as we described previously (53). Briefly, poly(A) mRNA from the total RNA was enriched using oligo(dT) beads. Following purification, fragmentation buffer was added to break mRNA into small pieces. Using these cleaved RNA fragments as the template, the first cDNA strand was synthesized by reverse transcription with random hexamer primers. The second-strand cDNA was synthesized using buffer, dinucleoside triphosphates (dNTPs), RNase H, and DNA polymerase I, and the sequencing library was constructed according to the manufacturer's instructions (Illumina, San Diego, CA, USA). The libraries were sequenced on the Illumina HiSeq 2000 apparatus (Beijing Genomics Institute, Shenzhen, China) to produce 50-bp paired-end reads. Prior to mapping to the *M. robertsii* reference genome and annotated genes, adaptor tags, unknown, or low-quality tags were filtered to get clean tags. To compare levels of gene expression between the WT and a mutant, the number of raw clean tags in each library was normalized to the number of reads per kilobase per million reads (RPKM) to normalize gene expression levels. DEGs were identified using a false-discovery rate (FDR) of $\leq$0.001 and a fold change of $\geq$2 as the threshold. To further characterize the biological functions and metabolic pathways of DEGs, the DEGs were subjected to a GO functional analysis (Blast2GO; BioBam Bioinformatics) (54). A GO enrichment analysis of functional significance uses a hypergeometric test to map all DEGs to terms in the GO database, looking for significantly enriched GO terms among the genes differentially expressed from those in the background genome.

To validate the DGE results, 18 candidate genes were analyzed by qRT-PCR. The selected genes and primers are listed in Table 2. RNA samples used for qRT-PCR were the same as those used for DGE sequencing. First-strand cDNA synthesis and qRT-PCR were performed as described above. Three technical replicates of qRT-PCR were performed for each biological replicate.

TABLE 2 Verification of DGE results by qRT-PCR analysis

Gene ID	Gene product description[a]	Primer sequence (5′–3′)	Value from[b]: DGE[c]	qRT-PCR[d]	DGE[e]	qRT-PCR[f]
MAA_06313	Developmental regulator *flbA*	ACTCCAAAGGGCATCACG CAACAAAGCGGCGGAATA	0.97	3.27	−0.02	−1.02
MAA_01254	Subtilisin-like serine protease	CGAACGATAGCCGTGGTC GAAAGCCGCATTGAGCAG	14.35	18.76	−1.50	−5.01
MAA_09336	Glutamine synthetase	CCGATTATTGACAACCACG AAGGCATTTCCGAGTCCA	1.26	4.46	0.55	2.10
MAA_04342	Zinc finger domain-containing protein	TTTCCAATCTACGACGACA AGTCCGATTGATGGTCTTC	2.37	5.96	0.56	4.21
MAA_06808	Secretion pathway protein Sls2/Rcy1	ACGGAGGCGGTTTGAAGA AATGTCGTCGCTTGTGGC	0.86	2.85	−1.41	−4.72
MAA_07188	FAD-binding protein	AACCTGGCTATTAAAGTCACGC CACCCGACTTGGCTTGGAC	5.87	14.30	−2.25	−3.62
MAA_02988	APSES transcription factor	GCAAGGCACCAACCCACT TGCTGCTCCGTAGGCTGA	2.03	3.12	1.05	4.41
MAA_02740	Chitin synthase A	TGCGAACAGGGAAACCAG GACCCGAGTTCGAGAAGAG	0.92	4.01	−0.44	−1.56
MAA_03529	MAPKK kinase	ACCGAAAGTCGTATGTATCCT CCACTGATTGTCATCCCAC	0.78	3.14	−0.17	−1.06
MAA_03342	Integral membrane protein	ACTGATGTTGTTGCGGTGAT AAATCTGCCAACCAAAGG	12.99	10.32	−3.43	−5.72
MAA_03181	Serine/threonine protein kinase domain protein	ATCTTCACATCTGGCACGAC GTTTCCGTGGGCAACATAC	0.85	2.76	0.02	1.01
MAA_03488	Guanine nucleotide-binding protein alpha-subunit	TCGTGGTGTTGAGGAGTG ATGCGGTAGGTCAAGTCG	0.43	1.15	−0.52	−1.09
MAA_02691	Conidiophore development protein HymA	GCGGCTGTCATCCTCTAT ATCGGCTGCTACCTCAA	0.29	1.42	−0.10	−1.03
MAA_03203	Catalase A	TTTGGCACCTTTCGTCTCC CAGTTGCCCTCTTGCGTGT	−3.68	−10.20	−1.16	−4.12
MAA_05842	rRNA-processing protein Efg-1	TTCAACCCAAAGCGTCAG TTTGTCCGAGACGGTAGAT	−3.01	−6.51	−1.52	−3.27
MAA_08075	Carboxylesterase, type B	ACCTCCAGTCGGAAACCT GGTGCTCGTTGGAGTCTTA	−6.76	−10.34	−3.33	−7.87
MAA_10232	Ankyrin repeat-containing protein	GTTTCACAAGAATCCTCCTC AACGGATTGACGAGATGACT	14.15	19.02	−1.12	−2.89
MAA_02493	Ribosomal protein L13	TCGCCTCGCCTATTCACG CCAGATCGGCTTGTGCTT	−1.85	−6.26	−0.03	−1.78

[a]APSES, ASM-1, Phd1, StuA, EFG1, and Sok2 family; MAPKK, mitogen-activated protein kinase kinase.
[b]Positive numbers indicate that the genes were upregulated; negative numbers indicate that the genes were downregulated.
[c]Log_2(FPKM of WT CO/FPKM of WT MY), where FPKM is fragments per kilobase of transcript per million mapped reads.
[d]Gene expression ratio of WT CO to WT MY.
[e]Log_2(FPKM of the Δ*dcl2* mutant CO/FPKM of the Δ*dcl2* mutant MY).
[f]Gene expression ratio of the Δ*dcl2* mutant CO to the Δ*dcl2* mutant MY.

Solexa sequencing and analysis of *M. robertsii* sRNAs. Total RNAs were extracted from mycelia of the WT and the Δ*dcl2* mutant grown in SDAY for 2.5 days at 25°C. RNA concentrations were then evaluated using an ND-1000 spectrophotometer (NanoDrop, USA). A 2-μg aliquot was enriched for sRNA using the polyethylene glycol 8000 (PEG 8000) precipitation method (55). First, low-molecular-weight RNA was isolated from the total RNA. Next, the sRNA segments between 18 and 30 nt were separated using denatured 15% polyacrylamide gel electrophoresis (PAGE) gels and ligated sequentially to specific adaptors at the 5′ and 3′ ends. Then, the products were reverse transcribed to cDNA using RT-PCR. PCR products (75-nt size range) were obtained after amplification of cDNA by a low number of PCR cycles (15 to 20 cycles). The purified PCR products were checked for amount and quality with an Agilent 2100 Bioanalyzer and sequenced with an Illumina genome analyzer (BGI, Shenzhen, China).

Sequencing and bioinformatic analysis were performed as we described previously (24). Briefly, the final clean reads were obtained by getting rid of the adaptor contaminants from the raw reads. The sRNA sequences were mapped to the *M. robertsii* genome using the Short Oligonucleotide Alignment Program (SOAP) (25, 56). We used the Rfam database to remove the sRNAs that originated from rRNA, tRNA, snRNA, and snoRNA. The prediction of milRNAs was carried out using an algorithm named MIREAP (http://sourceforge.net/projects/mireap), which could identify all candidate precursors with canonical hairpin structures that were perfectly mapped by sequencing data.

Accession number(s). The mRNA raw sequence data were deposited in NCBI's GEO database (http://www.ncbi.nlm.nih.gov/geo/) with the accession no. GSE80731.

SUPPLEMENTAL MATERIAL

Supplemental material for this article may be found at https://doi.org/10.1128/AEM.03230-16.

SUPPLEMENTAL FILE 1, PDF file, 0.8 MB.
SUPPLEMENTAL FILE 2, XLS file, 1.1 MB.
SUPPLEMENTAL FILE 3, XLS file, 0.1 MB.
SUPPLEMENTAL FILE 4, XLSX file, 1.4 MB.

ACKNOWLEDGMENTS

We thank Chengshu Wang for providing fungus material and gene deletion vectors.

This work was supported by the National Natural Science Foundation of China (grants 31272096, 31471821, and 31572060), the Anhui Provincial Natural Science Foundation (grants 1308085QC61 and 1408085MKL37), and the Natural Science Foundation of the Higher Education Institutions of Anhui Province (grants KJ2015A081).

REFERENCES

1. Catalanotto C, Nolan T, Cogoni C. 2006. Homology effects in *Neurospora crassa*. FEMS Microbiol Lett 254:182–189. https://doi.org/10.1111/j.1574-6968.2005.00037.x.
2. Meister G, Tuschl T. 2004. Mechanisms of gene silencing by double-stranded RNA. Nature 431:343–349. https://doi.org/10.1038/nature02873.
3. Dang Y, Yang Q, Xue Z, Liu Y. 2011. RNA interference in fungi: pathways, functions, and applications. Eukaryot Cell 10:1148–1155. https://doi.org/10.1128/EC.05109-11.
4. Nakayashiki H, Kadotani N, Mayama S. 2006. Evolution and diversification of RNA silencing proteins in fungi. J Mol Evol 63:127–135. https://doi.org/10.1007/s00239-005-0257-2.
5. Kapoor M, Arora R, Lama T, Nijhawan A, Khurana JP, Tyagi AK, Kapoor S. 2008. Genome-wide identification, organization and phylogenetic analysis of Dicer-like, Argonaute and RNA-dependent RNA polymerase gene families and their expression analysis during reproductive development and stress in rice. BMC Genomics 9:451. https://doi.org/10.1186/1471-2164-9-451.
6. Zamore PD, Tuschl T, Sharp PA, Bartel DP. 2000. RNAi: double-stranded RNA directs the ATP-dependent cleavage of mRNA at 21 to 23 nucleotide intervals. Cell 101:25–33. https://doi.org/10.1016/S0092-8674(00)80620-0.
7. Bernstein E, Caudy AA, Hammond SM, Hannon GJ. 2001. Role for a bidentate ribonuclease in the initiation step of RNA interference. Nature 409:363–366. https://doi.org/10.1038/35053110.
8. Tang G, Reinhart BJ, Bartel DP, Zamore PD. 2003. A biochemical framework for RNA silencing in plants. Gene Dev 17:49–63. https://doi.org/10.1101/gad.1048103.
9. Nelson P, Kiriakidou M, Sharma A, Maniataki E, Mourelatos Z. 2003. The microRNA world: small is mighty. Trends Biochem Sci 28:534–540. https://doi.org/10.1016/j.tibs.2003.08.005.
10. Ding SW, Voinnet O. 2007. Antiviral immunity directed by small RNAs. Cell 130:413–426. https://doi.org/10.1016/j.cell.2007.07.039.
11. Fabian MR, Sonenberg N, Filipowicz W. 2010. Regulation of mRNA translation and stability by microRNAs. Annu Rev Biochem 79:351–379. https://doi.org/10.1146/annurev-biochem-060308-103103.
12. Siomi MC, Saito K, Siomi H. 2008. How selfish retrotransposons are silenced in Drosophila germline and somatic cells. FEBS Lett 582:2473–2478. https://doi.org/10.1016/j.febslet.2008.06.018.
13. Klattenhoff C, Theurkauf W. 2008. Biogenesis and germline functions of piRNAs. Development 135:3–9. https://doi.org/10.1242/dev.006486.
14. Carmell MA, Xuan Z, Zhang MQ, Hannon GJ. 2002. The Argonaute family: tentacles that reach into RNAi, developmental control, stem cell maintenance, and tumorigenesis. Gene Dev 16:2733–2742. https://doi.org/10.1101/gad.1026102.
15. He L, Hannon GJ. 2004. MicroRNAs: small RNAs with a big role in gene regulation. Nat Rev Genet 5:522–531. https://doi.org/10.1038/nrg1379.
16. Tijsterman M, Plasterk RHA. 2004. Dicers at RISC: the mechanism of RNAi. Cell 117:1–3. https://doi.org/10.1016/S0092-8674(04)00293-4.
17. Li L, Chang SS, Liu Y. 2010. RNA interference pathways in filamentous fungi. Cell Mol Life Sci 67:3849–3863. https://doi.org/10.1007/s00018-010-0471-y.
18. Chang SS, Zhang Z, Liu Y. 2012. RNA interference pathways in fungi: mechanisms and functions. Annu Rev Microbiol 66:305–323. https://doi.org/10.1146/annurev-micro-092611-150138.
19. Villalobos-Escobedo JM, Herrera-Estrella A, Carreras-Villasenor N. 2016. The interaction of fungi with the environment orchestrated by RNAi. Mycologia 108:556–571. https://doi.org/10.3852/15-246.
20. Liu J, Cao Y, Xia Y. 2010. Mmc, a gene involved in microcycle conidiation of the entomopathogenic fungus *Metarhizium anisopliae*. J Invertebr Pathol 105:132–138. https://doi.org/10.1016/j.jip.2010.05.012.
21. Cao Y, Li M, Xia Y. 2011. Mapmi gene contributes to stress tolerance and virulence of the entomopathogenic fungus, *Metarhizium acridum*. J Invertebr Pathol 108:7–12. https://doi.org/10.1016/j.jip.2011.06.002.
22. Leng Y, Peng G, Cao Y, Xia Y. 2011. Genetically altering the expression of neutral trehalase gene affects conidiospore thermotolerance of the entomopathogenic fungus *Metarhizium acridum*. BMC Microbiol 11:32. https://doi.org/10.1186/1471-2180-11-32.
23. Tiago PV, Fungaro MH, de Faria MR, Furlaneto MC. 2004. Effects of double-stranded RNA in *Metarhizium anisopliae* var. *acridum* and *Paecilomyces fumosoroseus* on protease activities, conidia production, and virulence. Can J Microbiol 50:335–339. https://doi.org/10.1139/w04-023.
24. Zhou Q, Wang Z, Zhang J, Meng H, Huang B. 2012. Genome-wide identification and profiling of microRNA-like RNAs from *Metarhizium anisopliae* during development. Fungal Biol 116:1156–1162. https://doi.org/10.1016/j.funbio.2012.09.001.
25. Gao Q, Jin K, Ying SH, Zhang Y, Xiao G, Shang Y, Duan Z, Hu X, Xie XQ, Zhou G, Peng G, Luo Z, Huang W, Wang B, Fang W, Wang S, Zhong Y, Ma LJ, St Leger RJ, Zhao GP, Pei Y, Feng MG, Xia Y, Wang C. 2011. Genome sequencing and comparative transcriptomics of the model entomopathogenic fungi *Metarhizium anisopliae* and *M. acridum*. PLoS Genet 7:e1001264. https://doi.org/10.1371/journal.pgen.1001264.
26. Hu Y, Stenlid J, Elfstrand M, Olson A. 2013. Evolution of RNA interference proteins Dicer and Argonaute in Basidiomycota. Mycologia 105:1489–1498. https://doi.org/10.3852/13-171.
27. Meng F, Jia H, Ling N, Xue Y, Liu H, Wang K, Yin J, Li Y. 2013. Cloning and characterization of two Argonaute genes in wheat (*Triticum aestivum* L.). BMC Plant Biol 13:18. https://doi.org/10.1186/1471-2229-13-18.
28. Bai M, Yang GS, Chen WT, Mao ZC, Kang HX, Chen GH, Yang YH, Xie BY. 2012. Genome-wide identification of Dicer-like, Argonaute and RNA-dependent RNA polymerase gene families and their expression analyses in response to viral infection and abiotic stresses in *Solanum lycopersicum*. Gene 501:52–62. https://doi.org/10.1016/j.gene.2012.02.009.
29. Qian Y, Cheng Y, Cheng X, Jiang H, Zhu S, Cheng B. 2011. Identification and characterization of Dicer-like, Argonaute and RNA-dependent RNA polymerase gene families in maize. Plant Cell Rep 30:1347–1363. https://doi.org/10.1007/s00299-011-1046-6.
30. Kadotani N, Nakayashiki H, Tosa Y, Mayama S. 2004. One of the two Dicer-like proteins in the filamentous fungi *Magnaporthe oryzae* genome is responsible for hairpin RNA-triggered RNA silencing and related small

interfering RNA accumulation. J Biol Chem 279:44467–44474. https://doi.org/10.1074/jbc.M408259200.
31. Lee YS, Nakahara K, Pham JW, Kim K, He Z, Sontheimer EJ, Carthew RW. 2004. Distinct roles for Drosophila Dicer-1 and Dicer-2 in the siRNA/miRNA silencing pathways. Cell 117:69–81. https://doi.org/10.1016/S0092-8674(04)00261-2.
32. Catalanotto C, Pallotta M, ReFalo P, Sachs MS, Vayssie L, Macino G, Cogoni C. 2004. Redundancy of the two dicer genes in transgene-induced posttranscriptional gene silencing in *Neurospora crassa*. Mol Cell Biol 24:2536–2545. https://doi.org/10.1128/MCB.24.6.2536-2545.2004.
33. de Haro JP, Calo S, Cervantes M, Nicolas FE, Torres-Martinez S, Ruiz-Vazquez RM. 2009. A single Dicer gene is required for efficient gene silencing associated with two classes of small antisense RNAs in *Mucor circinelloides*. Eukaryot Cell 8:1486–1497. https://doi.org/10.1128/EC.00191-09.
34. Carreras-Villaseñor N, Esquivel-Naranjo EU, Villalobos-Escobedo JM, Abreu-Goodger C, Herrera-Estrella A. 2013. The RNAi machinery regulates growth and development in the filamentous fungus *Trichoderma atroviride*. Mol Microbiol 89:96–112. https://doi.org/10.1111/mmi.12261.
35. Cao Y, Du M, Luo S, Xia Y. 2014. Calcineurin modulates growth, stress tolerance, and virulence in *Metarhizium acridum* and its regulatory network. Appl Microbiol Biotechnol 98:8253–8265. https://doi.org/10.1007/s00253-014-5876-3.
36. Twumasi-Boateng K, Yu Y, Chen D, Gravelat FN, Nierman WC, Sheppard DC. 2009. Transcriptional profiling identifies a role for BrlA in the response to nitrogen depletion and for StuA in the regulation of secondary metabolite clusters in *Aspergillus fumigatus*. Eukaryot Cell 8:104–115. https://doi.org/10.1128/EC.00265-08.
37. Park HS, Yu J-H. 2012. Genetic control of asexual sporulation in filamentous fungi. Curr Opin Microbiol 15:669–677. https://doi.org/10.1016/j.mib.2012.09.006.
38. Sigl C, Haas H, Specht T, Pfaller K, Kurnsteiner H, Zadra I. 2011. Among developmental regulators, StuA but not BrlA is essential for penicillin V production in *Penicillium chrysogenum*. Appl Environ Microbiol 77:972–982. https://doi.org/10.1128/AEM.01557-10.
39. Adams TH, Wieser JK, Yu JH. 1998. Asexual sporulation in *Aspergillus nidulans*. Microbiol Mol Biol Rev 62:35–54.
40. Lee HC, Li L, Gu W, Xue Z, Crosthwaite SK, Pertsemlidis A, Lewis ZA, Freitag M, Selker EU, Mello CC, Liu Y. 2010. Diverse pathways generate microRNA-like RNAs and Dicer-independent small interfering RNAs in fungi. Mol Cell 38:803–814. https://doi.org/10.1016/j.molcel.2010.04.005.
41. Bühler M, Spies N, Bartel DP, Moazed D. 2008. TRAMP-mediated RNA surveillance prevents spurious entry of RNAs into the *Schizosaccharomyces pombe* siRNA pathway. Nat Struct Mol Biol 15:1015–1023. https://doi.org/10.1038/nsmb.1481.
42. Lee HC, Chang SS, Choudhary S, Aalto AP, Maiti M, Bamford DH, Liu Y. 2009. qiRNA is a new type of small interfering RNA induced by DNA damage. Nature 459:274–277. https://doi.org/10.1038/nature08041.
43. Liu T, Hu J, Zuo Y, Jin Y, Hou J. 2015. Identification of microRNA-like RNAs from *Curvularia lunata* associated with maize leaf spot by bioinformation analysis and deep sequencing. Mol Genet Genomics 291:587–596. https://doi.org/10.1007/s00438-015-1128-1.
44. Bai Y, Lan F, Yang W, Zhang F, Yang K, Li Z, Gao P, Wang S. 2015. sRNA profiling in *Aspergillus flavus* reveals differentially expressed miRNA-like RNAs response to water activity and temperature. Fungal Genet Biol 81:113–119. https://doi.org/10.1016/j.fgb.2015.03.004.
45. Chen Y, Gao Q, Huang M, Liu Y, Liu Z, Liu X, Ma Z. 2015. Characterization of RNA silencing components in the plant pathogenic fungus *Fusarium graminearum*. Sci Rep 5:12500. https://doi.org/10.1038/srep12500.
46. Thompson JD, Higgins DG, Gibson JT. 1994. CLUSTAL W: improving the sensitivity of progressive multiple sequence alignment through sequence weighting, position-specific gap penalties and weight matrix choice. Nucleic Acids Res 22:4673–4680. https://doi.org/10.1093/nar/22.22.4673.
47. Kumar S, Tamura K, Nei M. 2004. MEGA3: integrated software for Molecular Evolutionary Genetics Analysis and sequence alignment. Brief Bioinform 5:150–163. https://doi.org/10.1093/bib/5.2.150.
48. Fang W, Bidochka MJ. 2006. Expression of genes involved in germination, conidiogenesis and pathogenesis in *Metarhizium anisopliae* using quantitative real-time RT-PCR. Mycol Res 110:1165–1171. https://doi.org/10.1016/j.mycres.2006.04.014.
49. Livak KJ, Schmittgen TD. 2001. Analysis of relative gene expression data using real-time quantitative PCR and the $2^{-\Delta\Delta CT}$ method. Methods 25:402–408. https://doi.org/10.1006/meth.2001.1262.
50. Wang C, St. Leger RJ. 2006. A collagenous protective coat enables *Metarhizium anisopliae* to evade insect immune responses. Proc Natl Acad Sci U S A 103:6647–6652. https://doi.org/10.1073/pnas.0601951103.
51. Huang W, Shang Y, Chen P, Gao Q, Wang C. 2015. MrpacC regulates sporulation, insect cuticle penetration and immune evasion in *Metarhizium robertsii*. Environ Microbiol 17:994–1008. https://doi.org/10.1111/1462-2920.12451.
52. Fang W, Pei Y, Bidochka MJ. 2006. Transformation of *Metarhizium anisopliae* mediated by *Agrobacterium tumefaciens*. Can J Microbiol 52:623–626. https://doi.org/10.1139/w06-014.
53. Wang ZX, Zhou XZ, Meng HM, Liu YJ, Zhou Q, Huang B. 2014. Comparative transcriptomic analysis of the heat stress response in the filamentous fungus *Metarhizium anisopliae* using RNA-Seq. Appl Microbiol Biotechnol 98:5589–5597. https://doi.org/10.1007/s00253-014-5763-y.
54. Ye J, Fang L, Zheng H, Zhang Y, Chen J, Zhang Z, Wang J, Li S, Li R, Bolund L, Wang J. 2006. WEGO: a web tool for plotting GO annotations. Nucleic Acids Res 34:W293–W297. https://doi.org/10.1093/nar/gkl031.
55. Lu C, Meyers BC, Green PJ. 2007. Construction of small RNA cDNA libraries for deep sequencing. Methods 43:110–117. https://doi.org/10.1016/j.ymeth.2007.05.002.
56. Li R, Yu C, Li Y, Lam TW, Yiu SM, Kristiansen K, Wang J. 2009. SOAP2: an improved ultrafast tool for short read alignment. Bioinformatics 25:1966–1967. https://doi.org/10.1093/bioinformatics/btp336.